Applied Mathematics and Computation 289 (2016) 159–171

Contents lists available at ScienceDirect

Applied Mathematics and Computation

journal homepage: www.elsevier.com/locate/amc

Solitary-wave solutions of the GRLW equation using septic B-spline collocation method

S. Battal Gazi Karakoç [a], Halil Zeybek [b,*]

[a] Department of Mathematics, Faculty of Science and Art, Nevsehir Haci Bektas Veli University, Nevsehir 50300, Turkey
[b] Department of Applied Mathematics, Faculty of Computer Science, Abdullah Gul University, Kayseri 38080, Turkey

ARTICLE INFO

MSC:
41A15
65L60
76B25

Keywords:
GRLW equation
Collocation method
Septic B-spline
Soliton
Solitary waves

ABSTRACT

In this work, solitary-wave solutions of the generalized regularized long wave (GRLW) equation are obtained by using septic B-spline collocation method with two different linearization techniques. To demonstrate the accuracy and efficiency of the numerical scheme, three test problems are studied by calculating the error norms L_2 and L_∞ and the invariants I_1, I_2 and I_3. A linear stability analysis based on the von Neumann method of the numerical scheme is also investigated. Consequently, our findings indicate that our numerical scheme is preferable to some recent numerical schemes.

1. Introduction

This study has focused on the following generalized regularized long wave (GRLW) equation:

$$U_t + U_x + p(p+1)U^p U_x - \mu U_{xxt} = 0, \tag{1}$$

with physical boundary conditions $U \to 0$ as $x \to \pm\infty$, where p is a positive integer, μ is positive constant, t is time and x is the space coordinate. In this study, boundary and initial conditions are chosen

$$\begin{aligned} &U(a,t) = 0, && U(b,t) = 0,\\ &U_x(a,t) = 0, && U_x(b,t) = 0,\\ &U_{xxx}(a,t) = 0, && U_{xxx}(b,t) = 0,\\ &U(x,0) = f(x), && a \le x \le b, \end{aligned} \tag{2}$$

where $f(x)$ is a localized disturbance inside the considered interval and will be determined later. In the fluid problems, U is related to the wave amplitude of the water surface or similar physical quantity. In the plasma applications, U is the negative of the electrostatic potential.

Firstly, Peregrine [1,2] and later Benjamin et al. [3] presented the GRLW equation as a model for small-amplitude long waves on the surface of water in a channel. GRLW equation derived from long waves propagating in the positive x-direction is related to the generalized Korteweg–de Vries (GKdV) equation and is based upon the regularized long wave (RLW) equation. These general equations are nonlinear wave equations with $(p+1)$th nonlinearity and have solitary solutions, which are pulse-like. These equations describe phenomena with weak nonlinearity and dispersion waves, including nonlinear

* Corresponding author. Tel.: +90 3522248800.
E-mail addresses: sbgkarakoc@nevsehir.edu.tr (S.B.G. Karakoç), halil.zeybek@agu.edu.tr (H. Zeybek).

http://dx.doi.org/10.1016/j.amc.2016.05.021
0096-3003/

transverse waves in shallow water, ion-acoustic and magnetohydrodynamic waves in plasma and phonon packets in nonlinear crystals. Therefore, the solitary-wave solution of the GRLW equation has an important role in understanding many physical phenomena.

Since 2000, both analytic and numerical solution methods have been used to solve the GRLW equation by many authors [4–19]. A finite difference scheme has been presented by Zhang [7]. Numerical solution of the GRLW equation has been obtained by Soliman [8] using He's variational iteration method. Mokhtari and Mohammadi [11] presented the Sinc-collocation method for this equation. Roshan [13] obtained the numerical solutions of the equation with Petrov–Galerkin method using a linear hat function as the trial function and a quintic B-spline function as the test function. Hammad and El-Azab [19] studied the equation using a 2N order compact finite difference method. In addition, recently, fully implicit space-time discontinuous Galerkin (DG) method has been proposed for obtaining the numerical solution of one-dimensional systems of advection–diffusion–dispersion–reaction equations, i.e. so-called Korteweg–de-Vries-type equations or Boussinesq-type equations by Dumbser and Facchini [34].

If $p = 1$ in Eq. (1), the obtained equation is known as the regularized long wave (RLW) equation. Until now, many researcher have solved the RLW equation by using various analytic and numerical methods. For instance, the RLW equation was solved using Galerkin method based on quadratic B-spline functions by Gardner et al. [20]. Raslan [21], Dağ et al. [22], Soliman and Hussien [23], Saka et al. [24,25] presented the quadratic, cubic, septic, quintic and sextic B-spline collocation method to find the numerical solution of the RLW equation. If $p = 2$, modified regularized long wave (MRLW) equation is obtained. The MRLW equation has been solved numerically by Gardner et al. [26] using B-spline finite elements. Cubic B-spline collocation method is investigated for solving the MRLW equation by Khalifa et al. [27]. Later on, finite elements method including quintic, quartic, extended cubic and septic B-spline collocation method has been used for solving the MRLW equation [28–32].

In the present paper, we have applied the septic B-spline collocation method using two different linearization techniques to the GRLW equation. This work is built as follows: in Section 2, numerical scheme is explained. A linear stability analysis is presented in Section 3. Numerical examples and results are given in Section 4. In the last section, Section 5, conclusion is presented.

2. Septic B-spline collocation method

We consider the solution region of the problem restricted over an interval $a \le x \le b$. The interval $[a, b]$ is partitioned into uniformly sized finite elements of length h by the knots x_m such that $a = x_0 < x_1 < \cdots < x_N = b$ and $h = \frac{b-a}{N}$. The set of septic B-spline functions $\{\phi_{-3}(x), \phi_{-2}(x), \ldots, \phi_{N+3}(x)\}$ forms a basis over the solution region $[a, b]$. The numerical solution $U_N(x, t)$ is written in terms of the septic B-splines as

$$U_N(x,t) = \sum_{m=-3}^{N+3} \phi_m(x)\delta_m(t), \tag{3}$$

where $\delta_m(t)$ are time dependent parameters and will be determined by using the boundary and collocation conditions. Septic B-splines $\phi_m(x)$, $(m = -3, -2, \ldots, N+3)$ at the knots x_m are defined over the interval $[a, b]$ by Prenter in 1975

$$\phi_m(x) = \frac{1}{h^7}\begin{cases} (x-x_{m-4})^7 & [x_{m-4}, x_{m-3}] \\ (x-x_{m-4})^7 - 8(x-x_{m-3})^7 & [x_{m-3}, x_{m-2}] \\ (x-x_{m-4})^7 - 8(x-x_{m-3})^7 + 28(x-x_{m-2})^7 & [x_{m-2}, x_{m-1}] \\ (x-x_{m-4})^7 - 8(x-x_{m-3})^7 + 28(x-x_{m-2})^7 - 56(x-x_{m-1})^7 & [x_{m-1}, x_m] \\ (x_{m+4}-x)^7 - 8(x_{m+3}-x)^7 + 28(x_{m+2}-x)^7 - 56(x_{m+1}-x)^7 & [x_m, x_{m+1}] \\ (x_{m+4}-x)^7 - 8(x_{m+3}-x)^7 + 28(x_{m+2}-x)^7 & [x_{m+1}, x_{m+2}] \\ (x_{m+4}-x)^7 - 8(x_{m+3}-x)^7 & [x_{m+2}, x_{m+3}] \\ (x_{m+4}-x)^7 & [x_{m+3}, x_{m+4}] \\ 0 & otherwise. \end{cases} \tag{4}$$

Each septic B-spline covers 8 elements, thus each element $[x_m, x_{m+1}]$ is covered by 8 splines. A typical finite interval $[x_m, x_{m+1}]$ is mapped to the interval [0, 1] by a local coordinate transformation defined by $h\xi = x - x_m$, $0 \le \xi \le 1$. So septic B-splines (4) in terms of ξ over [0, 1] can be defined as follows:

$$\begin{aligned} \phi_{m-3} &= 1 - 7\xi + 21\xi^2 - 35\xi^3 + 35\xi^4 - 21\xi^5 + 7\xi^6 - \xi^7, \\ \phi_{m-2} &= 120 - 392\xi + 504\xi^2 - 280\xi^3 + 84\xi^5 - 42\xi^6 + 7\xi^7, \\ \phi_{m-1} &= 1191 - 1715\xi + 315\xi^2 + 665\xi^3 - 315\xi^4 - 105\xi^5 + 105\xi^6 - 21\xi^7, \\ \phi_m &= 2416 - 1680\xi + 560\xi^4 - 140\xi^6 + 35\xi^7, \\ \phi_{m+1} &= 1191 + 1715\xi + 315\xi^2 - 665\xi^3 - 315\xi^4 + 105\xi^5 + 105\xi^6 - 35\xi^7, \end{aligned}$$

$$\phi_{m+2} = 120 + 392\xi + 504\xi^2 + 280\xi^3 - 84\xi^5 - 42\xi^6 + 21\xi^7,$$
$$\phi_{m+3} = 1 + 7\xi + 21\xi^2 + 35\xi^3 + 35\xi^4 + 21\xi^5 + 7\xi^6 - \xi^7,$$
$$\phi_{m+4} = \xi^7. \tag{5}$$

For the problem, the finite elements are identified with the interval $[x_m, x_{m+1}]$. Using the expansion (3) and trial function (4), the nodal values of U_m, U'_m, U''_m, U'''_m are given in terms of the element parameters δ_m by

$$\begin{aligned} U_N(x_m,t) = U_m &= \delta_{m-3} + 120\delta_{m-2} + 1191\delta_{m-1} + 2416\delta_m + 1191\delta_{m+1} + 120\delta_{m+2} + \delta_{m+3},\\ U'_m &= \frac{7}{h}(-\delta_{m-3} - 56\delta_{m-2} - 245\delta_{m-1} + 245\delta_{m+1} + 56\delta_{m+2} + \delta_{m+3}),\\ U''_m &= \frac{42}{h^2}(\delta_{m-3} + 24\delta_{m-2} + 15\delta_{m-1} - 80\delta_m + 15\delta_{m+1} + 24\delta_{m+2} + \delta_{m+3}),\\ U'''_m &= \frac{210}{h^3}(-\delta_{m-3} - 8\delta_{m-2} + 19\delta_{m-1} - 19\delta_{m+1} + 8\delta_{m+2} + \delta_{m+3}), \end{aligned} \tag{6}$$

and the variation of U over the element $[x_m, x_{m+1}]$ is given by

$$U = \sum_{m=-3}^{N+3} \phi_m \delta_m. \tag{7}$$

Now, we identify the collocation points with the knots and use Eq. (6) to evaluate U_m, its space derivatives and substitute into Eq. (1) to obtain the set of the coupled ordinary differential equations: for the first linearization technique, we get the following equation:

$$\begin{aligned} &\dot\delta_{m-3} + 120\dot\delta_{m-2} + 1191\dot\delta_{m-1} + 2416\dot\delta_m + 1191\dot\delta_{m+1} + 120\dot\delta_{m+2} + \dot\delta_{m+3}\\ &+ \frac{7}{h}(-\delta_{m-3} - 56\delta_{m-2} - 245\delta_{m-1} + 245\delta_{m+1} + 56\delta_{m+2} + \delta_{m+3})\\ &+ \frac{7p(p+1)Z_m}{h}(-\delta_{m-3} - 56\delta_{m-2} - 245\delta_{m-1} + 245\delta_{m+1} + 56\delta_{m+2} + \delta_{m+3})\\ &- \frac{42\mu}{h^2}(\dot\delta_{m-3} + 24\dot\delta_{m-2} + 15\dot\delta_{m-1} - 80\dot\delta_m + 15\dot\delta_{m+1} + 24\dot\delta_{m+2} + \dot\delta_{m+3}) = 0, \end{aligned} \tag{8}$$

where

$$Z_m = (U_m)^p = (\delta_{m-3} + 120\delta_{m-2} + 1191\delta_{m-1} + 2416\delta_m + 1191\delta_{m+1} + 120\delta_{m+2} + \delta_{m+3})^p.$$

For the second (Rubin and Graves) linearization technique, we obtain the following general form of the solution method:

$$\begin{aligned} &\dot\delta_{m-3} + 120\dot\delta_{m-2} + 1191\dot\delta_{m-1} + 2416\dot\delta_m + 1191\dot\delta_{m+1} + 120\dot\delta_{m+2} + \dot\delta_{m+3}\\ &+ \frac{7}{h}(-\delta_{m-3} - 56\delta_{m-2} - 245\delta_{m-1} + 245\delta_{m+1} + 56\delta_{m+2} + \delta_{m+3})\\ &+ p(p+1)Z_m(\delta_{m-3} + 120\delta_{m-2} + 1191\delta_{m-1} + 2416\delta_m + 1191\delta_{m+1} + 120\delta_{m+2} + \delta_{m+3})\\ &- \frac{42\mu}{h^2}(\dot\delta_{m-3} + 24\dot\delta_{m-2} + 15\dot\delta_{m-1} - 80\dot\delta_m + 15\dot\delta_{m+1} + 24\dot\delta_{m+2} + \dot\delta_{m+3}) = 0, \end{aligned} \tag{9}$$

where

$$Z_m = (U_m)^{p-1}(U_m)_x$$

and $\cdot$ denotes derivative with respect to time. If time parameters δ_i and its time derivatives $\dot\delta_i$ in Eqs. (8) and (9) are discretized by the Crank–Nicolson formula and usual finite difference approximation, respectively,

$$\delta_m = \frac{1}{2}(\delta_m^n + \delta_m^{n+1}), \quad \dot\delta_m = \frac{\delta_m^{n+1} - \delta_m^n}{\Delta t} \tag{10}$$

for the first linearization, we obtain a recurrence relationship between two time levels n and $n+1$ relating two unknown parameters δ_i^{n+1}, δ_i^n for $i = m-3, m-2, \ldots, m+2, m+3$

$$\begin{aligned} &\gamma_1\delta_{m-3}^{n+1} + \gamma_2\delta_{m-2}^{n+1} + \gamma_3\delta_{m-1}^{n+1} + \gamma_4\delta_m^{n+1} + \gamma_5\delta_{m+1}^{n+1} + \gamma_6\delta_{m+2}^{n+1} + \gamma_7\delta_{m+3}^{n+1}\\ &= \gamma_7\delta_{m-3}^{n} + \gamma_6\delta_{m-2}^{n} + \gamma_5\delta_{m-1}^{n} + \gamma_4\delta_m^{n} + \gamma_3\delta_{m+1}^{n} + \gamma_2\delta_{m+2}^{n} + \gamma_1\delta_{m+3}^{n}, \end{aligned} \tag{11}$$

where

$$\begin{aligned} \gamma_1 &= (1 - E - p(p+1)EZ_m - M), & \gamma_2 &= (120 - 56E - 56p(p+1)EZ_m - 24M),\\ \gamma_3 &= (1191 - 245E - 245p(p+1)EZ_m - 15M), & \gamma_4 &= (2416 + 80M),\\ \gamma_5 &= (1191 + 245E + 245p(p+1)EZ_m - 15M), & \gamma_6 &= (120 + 56E + 56p(p+1)EZ_m - 24M), \end{aligned}$$

$$\gamma_7 = (1 + E + p(p+1)EZ_m - M),$$
$$m = 0, 1, \ldots, N, \quad E = \frac{7}{2h}\Delta t, \quad M = \frac{42\mu}{h^2}. \tag{12}$$

For the second (Rubin and Graves) linearization technique, the recurrence relationship has been obtained as follows

$$\beta_1\delta_{m-3}^{n+1} + \beta_2\delta_{m-2}^{n+1} + \beta_3\delta_{m-1}^{n+1} + \beta_4\delta_m^{n+1} + \beta_5\delta_{m+1}^{n+1} + \beta_6\delta_{m+2}^{n+1} + \beta_7\delta_{m+3}^{n+1} = \beta_8\delta_{m-3}^{n} + \beta_9\delta_{m-2}^{n} + \beta_{10}\delta_{m-1}^{n} + \beta_{11}\delta_m^{n} + \beta_{12}\delta_{m+1}^{n} + \beta_{13}\delta_{m+2}^{n} + \beta_{14}\delta_{m+3}^{n}, \tag{13}$$

where

$$\beta_1 = (1 - E + KZ_m - M), \qquad \beta_2 = (120 - 56E + 120KZ_m - 24M),$$
$$\beta_3 = (1191 - 245E + 1191KZ_m - 15M), \qquad \beta_4 = (2416 + 2416KZ_m + 80M),$$
$$\beta_5 = (1191 + 245E + 1191KZ_m - 15M), \qquad \beta_6 = (120 + 56E + 120KZ_m - 24M),$$
$$\beta_7 = (1 + E + KZ_m - M),$$
$$\beta_8 = (1 + E - KZ_m - M), \qquad \beta_9 = (120 + 56E - 120KZ_m - 24M),$$
$$\beta_{10} = (1191 + 245E - 1191KZ_m - 15M), \qquad \beta_{11} = (2416 - 2416KZ_m + 80M),$$
$$\beta_{12} = (1191 - 245E - 1191KZ_m - 15M), \qquad \beta_{13} = (120 - 56E - 120KZ_m - 24M),$$
$$\beta_{14} = (1 - E - KZ_m - M),$$
$$m = 0, 1, \ldots, N, \quad E = \frac{7}{2h}\Delta t, \quad K = \frac{p(p+1)}{2}\Delta t, \quad M = \frac{42\mu}{h^2}. \tag{14}$$

In the first linearization technique, the U^p term in non-linear term U^pU_x is taken as

$$Z_m = (U_m)^p = (\delta_{m-3} + 120\delta_{m-2} + 1191\delta_{m-1} + 2416\delta_m + 1191\delta_{m+1} + 120\delta_{m+2} + \delta_{m+3})^p. \tag{15}$$

In the second (Rubin and Graves) linearization technique, the $U^{p-1}U_x$ term in non-linear term U^pU_x is taken as

$$Z_m = (U_m)^{p-1}(U_m)_x. \tag{16}$$

When the Rubin and Graves [33] linearization technique is applied to the $U^{p-1}U_x$ term, we get the following equality

$$(U^{p-1}U_x)^{n+1} = (U^{p-1})^n(U_x)^{n+1} + (U^{p-1})^{n+1}(U_x)^n - (U^{p-1})^n(U_x)^n. \tag{17}$$

The system (11) and (13) consist of $(N+1)$ linear equations including $(N+7)$ unknown parameters $(\delta_{-3}, \delta_{-2}, \delta_{-1}, \ldots, \delta_{N+1}, \delta_{N+2}, \delta_{N+3})^T$. In order to obtain a unique solution for this system, we need six additional constraints. These are obtained from the boundary conditions (2) and can be used to eliminate $\delta_{-3}, \delta_{-2}, \delta_{-1}$ and $\delta_{N+1}, \delta_{N+2}, \delta_{N+3}$ from the systems (11) and (13) which then becomes a matrix equation for the $N+1$ unknowns $d^n = (\delta_0, \delta_1, \ldots, \delta_N)^T$ of the form

$$A\mathbf{d^{n+1}} = B\mathbf{d^n}. \tag{18}$$

The matrices A and B are $(N+1)\times(N+1)$ septa-diagonal matrices and this matrix equation can be solved by using the septa-diagonal algorithm.

Two or three inner iterations are applied to the term $\delta^{n*} = \delta^n + \frac{1}{2}(\delta^n - \delta^{n-1})$ at each time step to cope with the non-linearity caused by Z_m. Before the commencement of the solution process, initial parameters d^0 must be determined by using the initial condition and following derivatives at the boundaries;

$$U_N(x,0) = U(x_m,0); \qquad m = 0, 1, 2, \ldots, N$$
$$(U_N)_x(a,0) = 0, \qquad (U_N)_x(b,0) = 0,$$
$$(U_N)_{xx}(a,0) = 0, \qquad (U_N)_{xx}(b,0) = 0,$$
$$(U_N)_{xxx}(a,0) = 0, \qquad (U_N)_{xxx}(b,0) = 0.$$

So we have the following matrix form for the initial vector d^0;

$$Wd^0 = b,$$

where

$$W = \begin{bmatrix}
1536 & 2712 & 768 & 24 & & & & & & & \\
\frac{82731}{81} & \frac{210568.5}{81} & \frac{104796}{81} & \frac{10063.5}{81} & 1 & & & & & & \\
\frac{9600}{81} & \frac{96597}{81} & \frac{195768}{81} & \frac{96474}{81} & 120 & 1 & & & & & \\
 & & \ddots & & & & & & & & \\
 & & & 1 & 120 & 1191 & 2416 & 1191 & 120 & 1 & \\
 & & & & 1 & 120 & \frac{96474}{81} & \frac{195768}{81} & \frac{96597}{81} & \frac{9600}{81} & \\
 & & & & & 1 & \frac{10063.5}{81} & \frac{104796}{81} & \frac{210568.5}{81} & \frac{82731}{81} & \\
 & & & & & & 24 & 768 & 2712 & 1536 &
\end{bmatrix}$$

$d^0 = (\delta_0, \delta_1, \delta_2, \ldots, \delta_{N-2}, \delta_{N-1}, \delta_N)^T$ and $b = (U(x_0,0), U(x_1,0), \ldots, U(x_{N-1},0), U(x_N,0))^T$.

3. A linear stability analysis

To apply the von Neumann stability analysis, the GRLW equation must be linearized by considering that the quantity U^p in the nonlinear term U^pU_x is locally constant. Substituting the Fourier mode $\delta_m^n = \xi^n e^{imkh}$ $(i = \sqrt{-1})$ in which k is a mode number and h is the element size, into the Eq. (11) gives the growth factor ξ of the form

$$\xi = \frac{a - ib}{a + ib},$$

where

$$a = \gamma_4 + (\gamma_5 + \gamma_3)\cos[hk] + (\gamma_6 + \gamma_2)\cos[2hk] + (\gamma_7 + \gamma_1)\cos[3hk],$$
$$b = (\gamma_5 - \gamma_3)\sin[hk] + (\gamma_6 - \gamma_2)\sin[2hk] + (\gamma_7 - \gamma_1)\sin[3hk].$$

The modulus of $|\xi|$ is 1, so the linearized scheme is unconditionally stable.

4. Numerical examples and results

To show the accuracy of the numerical scheme and to compare our results with both exact values and other results given in the literature, the L_2 and L_∞ error norms are calculated by using the analytical solution in (19). Three test problems including: motion of a single solitary wave, interaction of two solitary waves and the Maxwellian initial condition are investigated. Furthermore, three invariants (20) are calculated in order to show the conservation properties of the numerical scheme. The error norms L_2 and L_∞ are given as follows:

$$L_2 = \left\| U^{exact} - U_N \right\|_2 \simeq \sqrt{h \sum_{J=0}^{N} \left| U_j^{exact} - (U_N)_j \right|^2},$$

and the error norm L_∞

$$L_\infty = \left\| U^{exact} - U_N \right\|_\infty \simeq \max_j \left| U_j^{exact} - (U_N)_j \right|.$$

The exact solution of GRLW Eq. (1) given in [26] is

$$U(x,t) = \sqrt[p]{\frac{c(p+2)}{2p}\sec h^2\left[\frac{p}{2}\sqrt{\frac{c}{\mu(c+1)}}(x - (c+1)t - x_0)\right]} \tag{19}$$

where c is the constant velocity of the wave travelling in the positive direction of the x-axis and x_0 is arbitrary constant. Three invariants of motion which correspond to conservation of mass, momentum and energy given in [26] are

$$I_1 = \int_a^b U dx, \quad I_2 = \int_a^b \left[U^2 + \mu U_x^2\right] dx, \quad I_3 = \int_a^b \left[U^4 - \mu U_x^2\right] dx. \tag{20}$$

4.1. The motion of single solitary wave

In this section, the invariants I_1, I_2, I_3 and the error norms L_2, L_∞ have been calculated by applying our numerical scheme using two different linearization techniques to Eq. (1). And then, our numerical results have been compared with the results given earlier [13,26,27]. The six sets of parameters have been constructed by taking different values of p, c, h, Δt and $amplitude = \sqrt[p]{\frac{c(p+2)}{2p}}$ and same values of $\mu = 1$, $x_0 = 40$, $0 \le x \le 100$.

In the first case, we consider $p = 2$, $c = 1$, $h = 0.2$, $\Delta t = 0.025$, so the solitary wave has $amplitude = 1$. The numerical computations are done up to $t = 10$. The obtained results are reported in Table 1 which shows that for the first linearization technique, three invariants are almost constant as the time progresses. For the second one, the changes of the invariants $I_1 \times 10^3$, $I_2 \times 10^3$ and $I_3 \times 10^3$ from their initial count are less than 0.0001, 0.2 and 0.2, respectively. Also, we observed that the quantity of the error norms L_2 and L_∞ obtained with second linearization technique are less than the obtained with first linearization technique.

In the second case, we select the parameters $p = 2$, $c = 0.3$, $h = 0.1$, $\Delta t = 0.01$, hence the solitary wave has $amplitude = 0.54772$. The numerical results are obtained from the time $t = 0$ to the time $t = 20$. The obtained results are given in Table 2 which shows that for the first linearization technique, three invariants are nearly constant as the time progresses. For the second one, the changes of the invariants $I_1 \times 10^5$, $I_2 \times 10^5$ and $I_3 \times 10^5$ from their initial state are less than 0.03, 0.2 and 0.2, respectively. If the magnitude of the error norms L_2 and L_∞ calculated using first and second linearization technique is compared, the magnitude for the second linearization technique is smaller than the first one.

Thirdly, if $p = 3$, $c = 6/5$, $h = 0.1$, $\Delta t = 0.025$, the solitary wave has $amplitude = 1$. The experiments are run from the time $t = 0$ to the time $t = 10$. The obtained results are tabulated in Table 3. It is observed from Table 3 that the changes of the invariants $I_1 \times 10^3$, $I_2 \times 10^3$ and $I_3 \times 10^3$ from their initial case are less than 0.06, 0.2 and 0.2, respectively. When we evaluate the error norms L_2 and L_∞ obtained using the first and second linearization, it is seen that the second linearization

Table 1
The invariants and the error norms for single solitary wave with $p = 2, amplitude = 1, c = 1,\ \Delta t = 0.025, h = 0.2, \mu = 1,\ 0 \le x \le 100$.

t		0	1	2	4	6	8	9	10
I_1	First	4.4428661	4.4428661	4.4428661	4.4428661	4.4428661	4.4428661	4.4428661	4.4428661
	Second	4.4428661	4.4428661	4.4428661	4.4428661	4.4428661	4.4428661	4.4428661	4.4428661
I_2	First	3.2998227	3.2998227	3.2998227	3.2998227	3.2998227	3.2998227	3.2998227	3.2998227
	Second	3.2998227	3.2998085	3.2997808	3.2997415	3.2997248	3.2997180	3.2997162	3.2997151
I_3	First	1.4142046	1.4142046	1.4142046	1.4142045	1.4142045	1.4142045	1.4142045	1.4142045
	Second	1.4142046	1.4142188	1.4142465	1.4142858	1.4143025	1.4143093	1.4143111	1.4143122
$L_2 \times 10^3$	First	0.00000000	0.31322962	0.60716949	1.14063868	1.64433340	2.13954492	2.38609516	2.63246332
	Second	0.00000000	0.28537793	0.56248008	1.08566992	1.58675627	2.08032250	2.32602024	2.57148152
$L_\infty \times 10^3$	First	0.00000000	0.20534214	0.36598695	0.63405702	0.88886854	1.14126892	1.26720221	1.39306406
	Second	0.00000000	0.16594258	0.31854916	0.58528925	0.83879372	1.08975930	1.21494581	1.34021078

Table 2
The invariants and the error norms for single solitary wave with $p = 2, amplitude = 0.54772, c = 0.3,\ \Delta t = 0.01, h = 0.1, \mu = 1,\ 0 \le x \le 100$.

t		0	2	4	8	12	16	18	20
I_1	First	3.5820205	3.5820205	3.5820205	3.5820205	3.5820206	3.5820205	3.5820205	3.5820204
	Second	3.5820205	3.5820205	3.5820205	3.5820205	3.5820206	3.5820206	3.5820205	3.5820204
I_2	First	1.3450941	1.3450941	1.3450941	1.3450941	1.3450941	1.3450941	1.3450941	1.3450941
	Second	1.3450941	1.3450942	1.3450945	1.3450949	1.3450952	1.3450954	1.3450955	1.3450956
I_3	First	0.1537283	0.1537283	0.1537283	0.1537283	0.1537283	0.1537283	0.1537283	0.1537283
	Second	0.1537283	0.1537282	0.1537280	0.1537275	0.1537272	0.1537270	0.1537269	0.1537268
$L_2 \times 10^4$	First	0.00000000	0.11808457	0.23672179	0.47619933	0.71790890	0.96089487	1.08268831	1.20462362
	Second	0.00000000	0.11675082	0.23418686	0.47177441	0.71193992	0.95355112	1.07469409	1.19599766
$L_\infty \times 10^4$	First	0.00000000	0.04821116	0.09872538	0.20175604	0.30567565	0.40978331	0.46185354	0.51392349
	Second	0.00000000	0.04844061	0.09904113	0.20198201	0.30544405	0.40924890	0.46114976	0.51304090

Table 3
The invariants and the error norms for single solitary wave with $p = 3, amplitude = 1, c = 6/5,\ \Delta t = 0.025, h = 0.1, \mu = 1,\ 0 \le x \le 100$.

t		0	1	2	4	6	8	9	10
I_1	First	3.7971850	3.7971850	3.7971850	3.7971850	3.7971850	3.7971850	3.7971850	3.7971850
	Second	3.7971850	3.7971799	3.7971746	3.7971643	3.7971539	3.7971436	3.7971385	3.7971333
I_2	First	2.8812522	2.8812522	2.8812522	2.8812522	2.8812522	2.8812522	2.8812522	2.8812522
	Second	2.8812523	2.8812352	2.8811910	2.8811373	2.8811139	2.8811003	2.8810949	2.8810899
I_3	First	0.9729661	0.9730414	0.9730958	0.9731319	0.9731417	0.9731447	0.9731453	0.9731457
	Second	0.9729661	0.9729832	0.9730274	0.9730811	0.9731045	0.9731181	0.9731235	0.9731285
$L_2 \times 10^3$	First	0.00000000	0.97308243	1.90329843	3.69133655	5.45488983	7.21419106	8.09357939	8.97298352
	Second	0.00000000	0.76815463	1.53511864	3.06287331	4.60591335	6.17668280	6.97351539	7.77816967
$L_\infty \times 10^3$	First	0.00000000	0.64473187	1.16955458	2.17410995	3.17420400	4.17483173	4.67535458	5.17598210
	Second	0.00000000	0.45766450	0.88908301	1.75051811	2.62846490	3.52598420	3.98164296	4.44187369

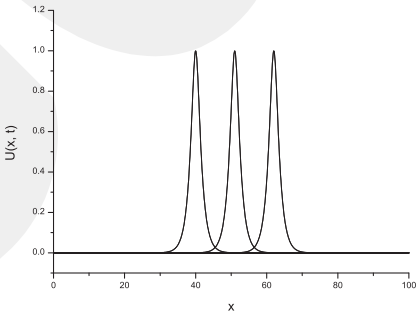

Fig. 1. Single solitary wave with $p = 3,\ c = 1.2,\ x_0 = 40,\ 0 \le x \le 100,\ t = 0, 5, 10$.

is better for our numerical scheme. Solitary wave profiles are depicted at different time levels in Fig. 1 in which the soliton moves to the right at a constant speed and nearly unchanged amplitude as time increases, as expected.

In the fourth case, we take $p = 3,\ c = 0.3,\ h = 0.1,\ \Delta t = 0.01$, so the solitary wave has $amplitude = 0.6$. The solutions are obtained until the time $t = 10$. The obtained results are reported in Table 4 which clearly shows that for the first linearization technique, three invariants are nearly unchanged as the time increases. For the second one, the changes of the invariants $I_1 \times 10^5$, $I_2 \times 10^5$ and $I_3 \times 10^5$ from their initial count are less than 0.02, 0.2 and 0.2, respectively. In addition,

Table 4
The invariants and the error norms for single solitary wave with $p = 3, amplitude = 0.6, c = 0.3,\ \Delta t = 0.01, h = 0.1, \mu = 1,\ 0 \le x \le 100$.

t		0	1	2	4	6	8	9	10
I_1	First	3.6776069	3.6776069	3.6776069	3.6776069	3.6776069	3.6776070	3.6776070	3.6776070
	Second	3.6776069	3.6776069	3.6776070	3.6776070	3.6776070	3.6776069	3.6776069	3.6776069
I_2	First	1.5657604	1.5657604	1.5657604	1.5657604	1.5657604	1.5657604	1.5657604	1.5657604
	Second	1.5657604	1.5657605	1.5657607	1.5657612	1.5657615	1.5657618	1.5657619	1.5657620
I_3	First	0.2268462	0.2268462	0.2268462	0.2268462	0.2268462	0.2268462	0.2268462	0.2268462
	Second	0.2268462	0.2268461	0.2268459	0.2268455	0.2268451	0.2268448	0.2268447	0.2268446
$L_2 \times 10^4$	First	0.00000000	0.08662190	0.17328588	0.34661331	0.52006829	0.69360491	0.78037511	0.86713653
	Second	0.00000000	0.07870034	0.15717557	0.31406200	0.47113473	0.62819930	0.70668688	0.78513671
$L_\infty \times 10^4$	First	0.00000000	0.04029558	0.08009713	0.15772492	0.23706868	0.31711953	0.35713873	0.39714589
	Second	0.00000000	0.03562449	0.07211019	0.14548091	0.21877988	0.29201943	0.32854583	0.36501241

Table 5
The invariants and the error norms for single solitary wave with $p = 4, amplitude = 1, c = 4/3,\ \Delta t = 0.025, h = 0.1, \mu = 1,\ 0 \le x \le 100$.

t		0	1	2	4	6	8	9	10
I_1	First	3.4687090	3.4687090	3.4687090	3.4687090	3.4687090	3.4687090	3.4687090	3.4687090
	Second	3.4687090	3.4687053	3.4687016	3.4686942	3.4686868	3.4686793	3.4686756	3.4686719
I_2	First	2.6716961	2.6716961	2.6716961	2.6716961	2.6716961	2.6716961	2.6716961	2.6716961
	Second	2.6716961	2.6716988	2.6716916	2.6716801	2.6716720	2.6716648	2.6716614	2.6716580
I_3	First	0.7291997	0.7292293	0.7292453	0.7292551	0.7292575	0.7292582	0.7292583	0.7292584
	Second	0.7291998	0.7291971	0.7292043	0.7292158	0.7292239	0.7292311	0.7292345	0.7292379
$L_2 \times 10^3$	First	0.00000000	0.34552640	0.68380580	1.35202774	2.01856221	2.68509298	3.01840343	3.35174007
	Second	0.00000000	0.23475400	0.47718681	0.98480922	1.52387541	2.09512659	2.39288065	2.69870907
$L_\infty \times 10^3$	First	0.00000000	0.22951531	0.43263300	0.83440039	1.24065060	1.64702738	1.84815798	2.04973389
	Second	0.00000000	0.15049211	0.29861347	0.60821892	0.93545672	1.28679533	1.46559601	1.65600236

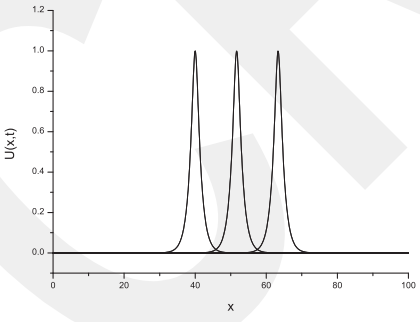

Fig. 2. Single solitary wave with $p = 4,\ c = 4/3,\ x_0 = 40,\ 0 \le x \le 100,\ t = 0, 5, 10$.

we observed that the quantity of the error norms L_2 and L_∞ obtained using second linearization technique are less than the ones obtained using first linearization technique.

When we choose the parameters $p = 4,\ c = 4/3,\ h = 0.1,\ \Delta t = 0.025,$ the solitary wave has $amplitude = 1$. The simulations are done up to $t = 10$. As can be seen in Table 5, the changes of the invariants $I_1 \times 10^4$, $I_2 \times 10^4$ and $I_3 \times 10^4$ from their initial value are less than 0.4. The values of the error norms L_2 and L_∞ in the second linearization are smaller than the first. Fig. 2 shows that our numerical scheme performs the soliton, which moves to the right at a constant speed and conserves its amplitude and shape with increasing time, as expected.

Finally, for the quantities $p = 4,\ c = 0.3,\ h = 0.1,\ \Delta t = 0.01,$ the solitary wave has $amplitude = 0.6$. The computer program is run until $t = 10$. The obtained results are listed in Table 6 which shows that for the first linearization technique, three invariants are nearly unchanged as the time processes. For the second one, the changes of the invariants $I_1 \times 10^5$, $I_2 \times 10^5$ and $I_3 \times 10^5$ from their initial quantity are less than 0.03, 0.3 and 0.3, respectively. By using the second linearization, we have found out that the quantity of the error norms L_2 and L_∞ is smaller than the ones.

In Table 7, the values of the invariants and error norms obtained by present scheme have been compared with the ones obtained by earlier methods at $t = 10$ [13,26,27]. Table 7 shows that our error norm values are smaller than the others. Also three invariant values have been observed to be close to each other.

Table 6
The invariants and the error norms for single solitary wave with $p = 4, amplitude = 0.6, c = 0.3,\ \Delta t = 0.01, h = 0.1, \mu = 1,\ 0 \le x \le 100$.

t		0	1	2	4	6	8	9	10
I_1	First	3.7592865	3.7592865	3.7592865	3.7592865	3.7592865	3.7592865	3.7592865	3.7592865
	Second	3.7592865	3.7592865	3.7592865	3.7592865	3.7592864	3.7592864	3.7592864	3.7592863
I_2	First	1.7300238	1.7300238	1.7300238	1.7300238	1.7300238	1.7300238	1.7300238	1.7300238
	Second	1.7300239	1.7300241	1.7300244	1.7300250	1.7300254	1.7300256	1.7300258	1.7300259
I_3	First	0.2894189	0.2894190	0.2894191	0.2894192	0.2894192	0.2894192	0.2894192	0.2894192
	Second	0.2894189	0.2894187	0.2894183	0.2894178	0.2894174	0.2894171	0.2894170	0.2894169
$L_2 \times 10^4$	First	0.00000000	0.12698867	0.25417530	0.50867400	0.76378746	1.01967310	1.14789286	1.27628477
	Second	0.00000000	0.10035765	0.19937853	0.39600506	0.59159317	0.78622772	0.88322868	0.98004530
$L_\infty \times 10^4$	First	0.00000000	0.06771033	0.13193138	0.25511505	0.37848569	0.50227119	0.56431519	0.62645346
	Second	0.00000000	0.04927491	0.09833776	0.19527926	0.29108460	0.38611041	0.43351464	0.48083798

Table 7
For $p = 2, 3$ and 4, comprasions of result for the single solitary wave with $\mu = 1, t = 10,\ 0 \le x \le 100$.

	p	2	3	4
		$c = 1, \Delta t = 0.025, h = 0.2$	$c = 0.3, \Delta t = 0.01, h = 0.1$	$c = 0.3, \Delta t = 0.01, h = 0.1$
	Collocation+PA-CN (cubic) [26]	4.44000000		
	Collocation-CN (cubic) [26]	4.44200000		
I_1	Collocation (cubic) [27]	4.44288000		
	Petrov–Galerkin (quintic) [13]	4.44288000	3.67755000	3.75923000
	Ours – Collocation (septic)	4.44286610	3.67760690	3.75928630
	Collocation+PA-CN (cubic) [26]	3.29600000		
	Collocation-CN (cubic) [26]	3.29900000		
I_2	Collocation (cubic) [27]	3.29983000		
	Petrov–Galerkin (quintic) [13]	3.29981000	1.56574000	1.72999000
	Ours – Collocation (septic)	3.29971510	1.56576200	1.73002590
	Collocation+PA-CN (cubic) [26]	1.41100000		
	Collocation-CN (cubic) [26]	1.41300000		
I_3	Collocation (cubic) [27]	1.41420000		
	Petrov–Galerkin (quintic) [13]	1.41416000	0.22683700	0.28940600
	Ours – Collocation (septic)	1.41431220	0.22684460	0.28941690
	Collocation+PA-CN (cubic) [26]	20.30000000		
	Collocation-CN (cubic) [26]	16.39000000		
$L_2 \times 10^3$	Collocation (cubic) [27]	9.30196000		
	Petrov–Galerkin (quintic) [13]	3.00533000	0.07197600	0.12253900
	Ours – Collocation (septic)	2.57148152	0.07851367	0.09800453
	Collocation+PA-CN (cubic) [26]	11.20000000		
	Collocation-CN (cubic) [26]	9.24000000		
$L_\infty \times 10^3$	Collocation (cubic) [27]	5.43718000		
	Petrov–Galerkin (quintic) [13]	1.68749000	0.03772280	0.06620700
	Ours – Collocation (septic)	1.34021078	0.03650124	0.04808379

4.2. The interaction of two solitary waves

In this section, we have focused on the interaction of two well separated solitary waves by using the following initial condition

$$U(x,0) = \sum_{i=1}^{2} \sqrt[p]{\frac{c_i(p+2)}{2p}\, \sec h^2\left[\frac{p}{2}\sqrt{\frac{c_i}{\mu(c_i+1)}}(x - x_i)\right]} \tag{21}$$

where c_i and x_i, $i = 1, 2$ are arbitrary constants. Eq. (21) represents two solitary waves having different amplitudes at the same direction. Three sets of parameters are considered.

In the first case, we choose $p = 2,\ c_1 = 4,\ c_2 = 1,\ x_1 = 25,\ x_2 = 55,\ h = 0.2,\ \Delta t = 0.025,\ \mu = 1,\ 0 \le x \le 250$. The experiments are run from $t = 0$ to $t = 20$. The values of the invariant quantities I_1, I_2 and I_3 are listed in Table 8 which shows that for the first linearization, the changes of the invariant $I_1 \times 10^6$, $I_2 \times 10^6$ and $I_3 \times 10^2$ from their initial case are less than 0.2, 0.4 and 0.5, respectively. The invariants are also found to be close to the ones obtained by using quintic Petrov–Galerkin method.

Secondly, we consider the parameters $p = 3,\ c_1 = 48/5,\ c_2 = 6/5,\ x_1 = 20,\ x_2 = 50,\ h = 0.1,\ \Delta t = 0.01,\ \mu = 1,\ 0 \le x \le 120$. The simulations are done up to time $t = 6$ to find the numerical invariants I_1, I_2 and I_3 at various time. The obtained results are reported in Table 9. From the table, it is observed that the numerical values of the invariants are found to be in good agreement with the quintic Petrov–Galerkin method [13] during the computer run. Fig. 3(a)–(d) illustrates the interaction of two solitary waves at different times. From this figure, we observed that at time $t = 0$, the wave with larger

Table 8
The invariants for interaction of two solitary waves with $p = 2, c_1 = 4, c_2 = 1, x_1 = 25, x_2 = 55,\ \Delta t = 0.025, h = 0.2, \mu = 1,\ 0 \le x \le 250$.

	t	0	2	4	8	12	16	18	20
	Ours – First	11.4676542	11.4676542	11.4676542	11.4676542	11.4676542	11.4676541	11.4676541	11.4676541
I_1	Ours – Second	11.4676542	11.4676503	11.4676484	11.4668849	11.4676777	11.4676555	11.4676490	11.4676452
	Pet.–Gal.(quint.)	11.4677000	11.4677000	11.4677000	11.4677000	11.4677000	11.4677000	11.4677000	11.4677000
	Ours – First	14.6292089	14.6292088	14.6292088	14.6292088	14.6292087	14.6292087	14.6292087	14.6292086
I_2	Ours – Second	14.6292089	14.6280240	14.6277880	14.1400014	14.6803731	14.6442435	14.6350836	14.6309639
	Pet.–Gal.(quint.)	14.6286000	14.6299000	14.6292000	14.6229000	14.6299000	14.6295000	14.6296000	14.6299000
	Ours – First	22.8803575	22.8803216	22.8803204	22.8759840	22.8803706	22.8803978	22.8803925	22.8803901
I_3	Ours – Second	22.8803575	22.8815424	22.8817784	23.3695650	22.8291933	22.8653229	22.8744828	22.8786025
	Pet.–Gal.(quint.)	22.8788000	22.8799000	22.8811000	22.8798000	22.8803000	22.8805000	22.8807000	22.8806000

Table 9
The invariants for interaction of two solitary waves with $p = 3, c_1 = 48/5, c_2 = 6/5, x_1 = 20, x_2 = 50,\ \Delta t = 0.01, h = 0.1, \mu = 1,\ 0 \le x \le 120$.

	t	0	1	2	3	4	5	6
	Ours – First	9.6907772	9.6907774	9.6907776	9.6907778	9.6907778	9.6907780	9.6907782
I_1	Ours – Second	9.6907772	9.6894501	9.6881175	9.6850972	9.6860154	9.6847993	9.6834620
	Pet.–Gal.(quint.)	9.6907500	9.6907400	9.6907400	9.6907400	9.6907400	9.6907400	9.6907400
	Ours – First	12.9443914	12.9443919	12.9443925	12.9443930	12.9443932	12.9443937	12.9443943
I_2	Ours – Second	12.9443914	12.9432906	12.9390629	12.3046064	12.9703128	13.0538036	13.0027533
	Pet.–Gal.(quint.)	12.9444000	12.9459000	12.9452000	12.9379000	12.9453000	12.9457000	12.9454000
	Ours – First	17.0186758	17.0236820	17.0256746	17.9687428	16.9816963	16.9181837	16.9520240
I_3	Ours – Second	17.0186758	17.0197766	17.0240043	17.6584608	16.9927544	16.9092637	16.9603139
	Pet.–Gal.(quint.)	17.0184000	16.9819000	16.9835000	17.0591000	16.9261000	16.8781000	16.9113000

Table 10
The invariants for interaction of two solitary waves with $p = 4, c_1 = 64/3, c_2 = 4/3, x_1 = 20, x_2 = 80,\ \Delta t = 0.01, h = 0.125, \mu = 1,\ 0 \le x \le 200$.

	t	0	1	2	3	4	5	6
	Ours – First	8.8342728	8.8342136	8.8341602	8.8341068	8.8340534	8.8340001	8.8339467
I_1	Ours – Second	8.8342728	8.6690235	8.5641864	8.4846626	8.4354647	8.3773932	8.3271616
	Pet.–Gal.(quint.)	8.8342700	8.8342700	8.8420400	8.8420500	8.8420900	8.8342100	8.8343400
	Ours – First	12.1708877	12.1707034	12.1705372	12.1703713	12.1702053	12.1700395	12.1698737
I_2	Ours – Second	12.1708877	12.0300916	11.9395989	11.8340526	11.9770970	11.9162211	11.8147229
	Pet.–Gal.(quint.)	12.1697000	12.3179000	12.3700000	12.4530000	12.5703000	12.6304000	12.6103000
	Ours – First	14.0294238	14.4197656	14.4134423	14.3841812	14.3516241	14.3210739	14.2929015
I_3	Ours – Second	14.0294238	14.1702200	14.2607126	14.3662589	14.2232145	14.2840904	14.3855886
	Pet.–Gal.(quint.)	14.0302000	13.8420000	13.9607000	14.0887000	13.9805000	14.2357000	14.6974000

amplitude is to the left of the second wave with smaller amplitude. As the time increases, overlapping process occurs. After the time $t = 3$, waves start to resume their original shapes.

Finally, we consider $p = 4$, $c_1 = 64/3$, $c_2 = 4/3$, $x_1 = 20$, $x_2 = 80$, $h = 0.125$, $\Delta t = 0.01$, $\mu = 1$, $0 \le x \le 200$. The computer program is run until time $t = 6$. To record the conservate quantities of the invariants I_1, I_2 and I_3, the calculated values are given in Table 10 which shows that the changes of the invariants $I_1 \times 10^2$, $I_2 \times 10^2$ and I_3 from their initial case are less than 0.03, 0.2 and 0.4, respectively. The invariants are almost same as those of Roshan. The motion of two solitary waves using our method is plotted at different time levels in Fig. 4(a)–(d). This figure shows that at time $t = 0$, the wave with larger amplitude is on the left of the second wave with smaller amplitude. In progress of time, interaction starts and overlapping process occurs. At the time $t = 6$, waves start to resume their original shapes.

4.3. A Maxwellian initial condition

As a last problem, we consider the Eq. (1) with the following Maxwellian initial condition

$$U(x, 0) = Exp(-x^2), \quad -20 \le x \le 60. \tag{22}$$

In this case, the behavior of the solution depends on the values of μ. Therefore, we chose the values of $\mu = 0.01$, $\mu = 0.025$, $\mu = 0.05$, $\mu = 0.1$ for $p = 2, 3, 4$. The numerical computations are done up to $t = 6$. The values of the three invariants of motion for different μ are presented in Table 11. The changes of the invariants $I_1 \times 10^2$, I_2 and I_3 from their initial values are less than 0.0001, 0.1 and 0.1 for $p = 2$; 0.0005, 0.2 and 0.2 for $p = 3$; 0.2, 0.3 and 0.3 for $p = 4$, respectively. The difference of the invariants between our method and quintic Petrov-Galerkin method is very little at the time $t = 6$. Also Fig. 5(a)–(d) and Fig. 6(a)–(d) illustrates the development of the Maxwellian initial condition into solitary waves. In

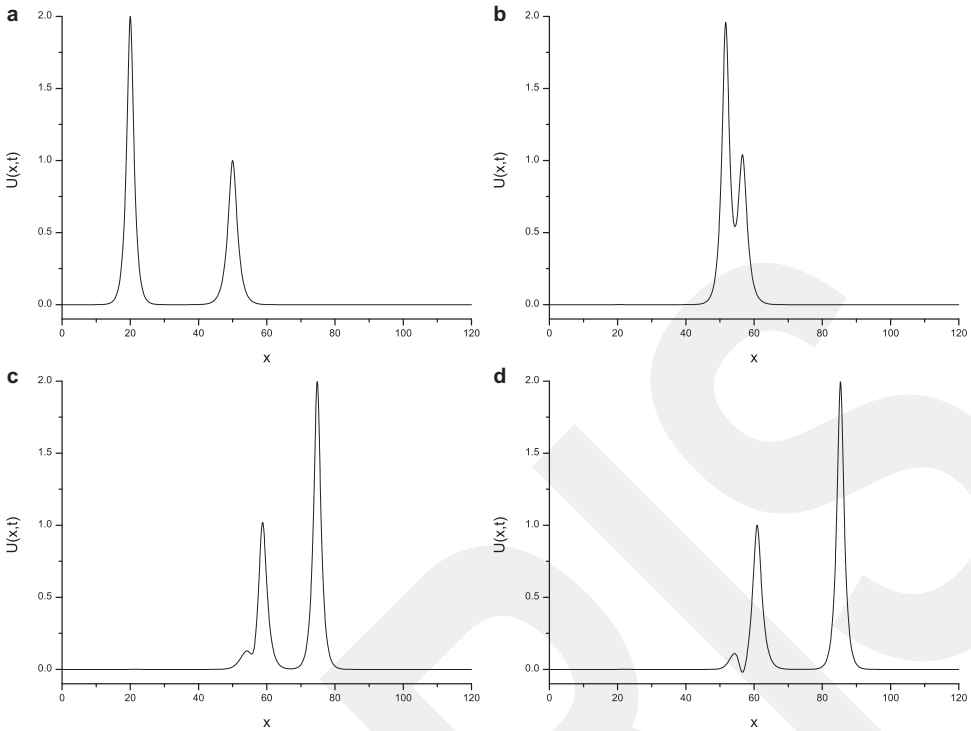

Fig. 3. Interaction of two solitary waves at $p = 3$; (a) $t = 0$, (b) $t = 3$, (c) $t = 5$, (d) $t = 6$.

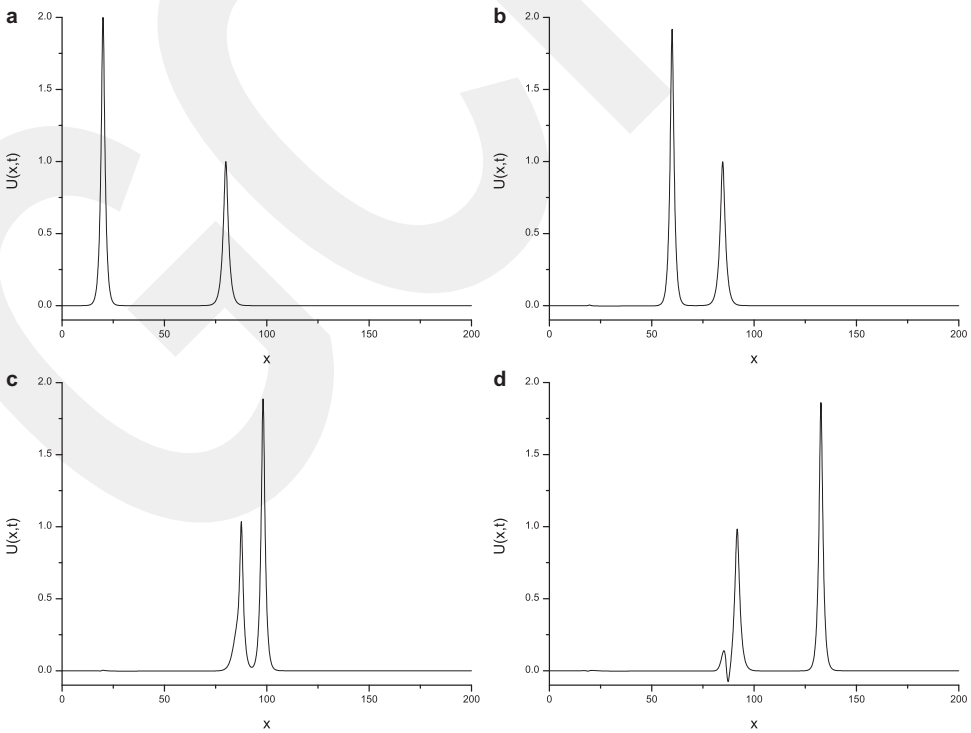

Fig. 4. Interaction of two solitary waves at $p = 4$; (a) $t = 0$, (b) $t = 2$, (c) $t = 4$, (d) $t = 6$.

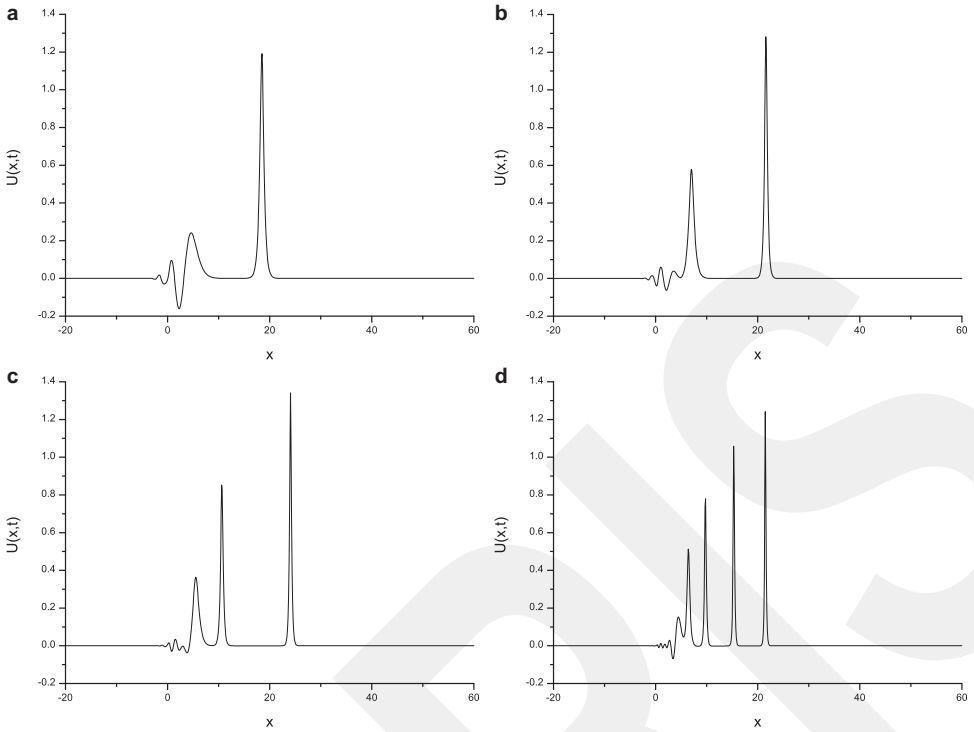

Fig. 5. Maxwellian initial condition $p = 3$ at $t = 6$; (a) $\mu = 0.1$, (b) $\mu = 0.05$, (c) $\mu = 0.025$, (d) $\mu = 0.01$.

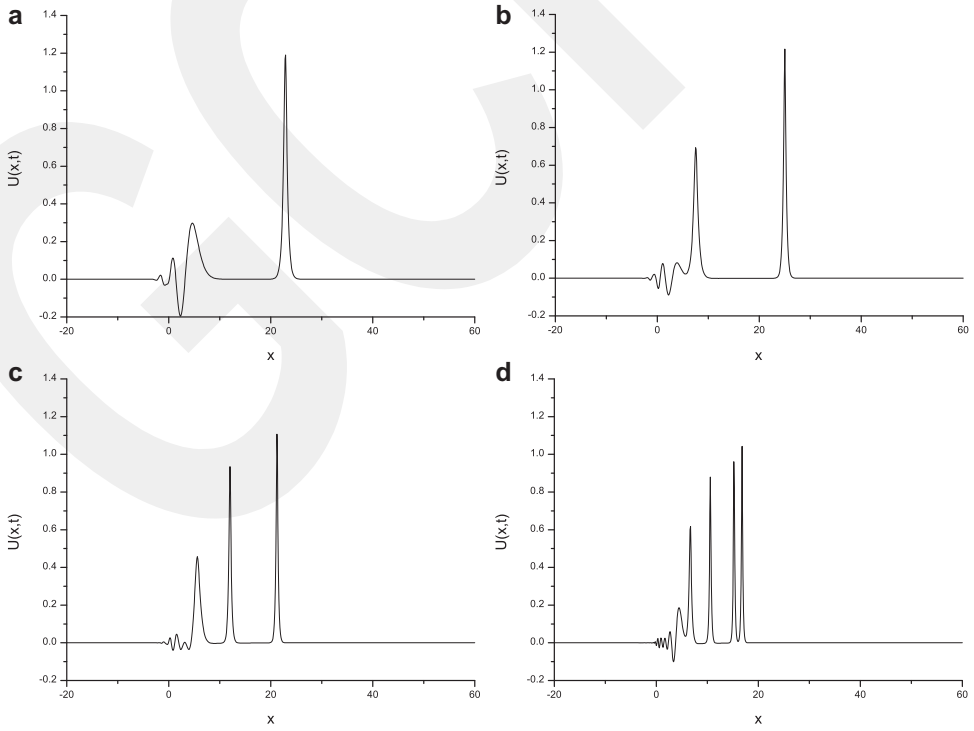

Fig. 6. Maxwellian initial condition $p = 4$ at $t = 6$; (a) $\mu = 0.1$, (b) $\mu = 0.05$, (c) $\mu = 0.025$, (d) $\mu = 0.01$.

Table 11
The invariants for Maxwellian initial condition.

μ	t	$p=2$			$p=3$			$p=4$		
		I_1	I_2	I_3	I_1	I_2	I_3	I_1	I_2	I_3
	0	1.772453	1.378645	0.760895	1.772453	1.378645	0.760895	1.772453	1.378645	0.760895
	2	1.772453	1.472878	0.666662	1.772452	1.548191	0.591349	1.772110	1.591837	0.547703
0.1	4	1.772453	1.472838	0.666702	1.772451	1.546329	0.593211	1.771702	1.588948	0.550592
	6	1.772453	1.472598	0.666942	1.772449	1.545540	0.594000	1.771297	1.587779	0.551761
Pet.–Gal.(qu.)	6	1.772450	1.380900	0.761900	1.772450	1.384330	0.599080	1.772450	1.389450	0.449163
	0	1.772453	1.315979	0.823561	1.772453	1.315979	0.823561	1.772453	1.315979	0.823561
	2	1.772453	1.457911	0.681630	1.772376	1.514843	0.624697	1.753662	1.535874	0.603666
0.05	4	1.772453	1.456986	0.682554	1.772272	1.514131	0.625409	1.741625	1.528679	0.610862
	6	1.772453	1.455748	0.683792	1.772168	1.513035	0.626505	1.733910	1.523490	0.616050
Pet.–Gal.(qu.)	6	1.772390	1.319510	0.825686	1.772480	1.323940	0.624720	1.772120	1.451680	0.489711
	0	1.772453	1.284646	0.854894	1.772453	1.284646	0.854894	1.772453	1.284646	0.854894
	2	1.772454	1.446475	0.693065	1.768943	1.502469	0.637071	1.693029	1.482414	0.657126
0.025	4	1.772452	1.450770	0.688770	1.764956	1.501801	0.637740	1.682425	1.476250	0.663290
	6	1.772451	1.450891	0.688649	1.761477	1.498994	0.640546	1.674869	1.468703	0.670837
Pet.–Gal.(qu.)	6	1.772380	1.290110	0.854909	1.772350	1.308060	0.635790	1.772490	1.296260	0.479621
	0	1.772453	1.265847	0.873693	1.772453	1.265847	0.873693	1.772453	1.265847	0.873693
	2	1.772512	1.438944	0.700596	1.720433	1.456451	0.683090	1.651315	1.437490	0.702051
0.01	4	1.772403	1.443961	0.695579	1.706008	1.450265	0.689276	1.644999	1.439995	0.699545
	6	1.772190	1.443723	0.695817	1.700567	1.451593	0.687947	1.633634	1.431710	0.707830
Pet.–Gal.(qu.)	6	1.772490	1.283150	0.892359	1.772450	1.276270	0.632880	1.756480	1.405770	0.381194

Figs. 5(a) and 6(a), the solitary wave with larger one is on the right of the smaller one. For $\mu = 0.1$, only single stable solition appeared. When $\mu = 0.05$, two stable solitary wave appeared in Figs. 5(b) and 6(b). As seen in Fig. 5(c) and (d) and Fig. 6(c) and (d), three and four stable solitary wave occurred at the $\mu = 0.025$ and $\mu = 0.01$, respectively. It is understood from these figures that as the value of μ decreases, the number of the stable solitary wave increases.

5. Conclusion

In this paper, we have constructed the numerical algorithm based on the septic B spline collocation method using two different linearization techniques for obtaining the solitary-wave solutions of the GRLW equation. The error norms L_2, L_∞ for single soliton and the invariants I_1 , I_2, I_3 for the three test problems including single soliton, interaction of solitons and Maxwellian initial condition have been calculated. The obtained results are tabulated. As seen from these tables, for each linearization technique, the changes of the invariants are reasonably small and the values of invariants are consistent with the other results. The quantity of obtained error norms are better than the ones in previous numerical methods. As a consequence, the presented numerical scheme is more preferable and more reliable for getting better numerical result of the physically important nonlinear partial differential equations.

Acknowledgments

The authors would like to express their sincere thanks to the reviewers for their careful reading, valuable comments and suggestions.

References

[1] D.H. Peregrine, Calculations of the development of an undular bore, J. Fluid Mech. 25 (2) (1966) 321–330.
[2] D.H. Peregrine, Long waves on a beach, J. Fluid Mech. 27 (4) (1967) 815–827.
[3] T.B. Benjamin, J.L. Bona, J.J. Mahony, Model equations for long waves in non-linear dispersive systems, Philos. Trans. R. Soc. Lond. Ser. A 272 (1972) 47–78.
[4] S. Hamdi, W.H. Enright, W.E. Schiesser, J.J. Gottlieb, Exact solutions and invariants of motion for general types of regularized long wave equations, Math. Comput. Simul. 65 (2004) 535–545.
[5] J.L. Bona, W.R. McKinney, J.M. Restrepo, Stable and unstable solitary-wave solutions of the generalized regularized long-wave equation, J. Nonlinear Sci. 10 (2000) 603–638, doi:10.1007/s003320010003.
[6] D. Kaya, A numerical simulation of solitary-wave solutions of the generalized regularized long-wave equation, Appl. Math. Comput. 149 (2004) 833–841, doi:10.1016/S0096-3003(03)00189-9.
[7] L. Zhang, A finite difference scheme for generalized regularized long-wave equation, Appl. Math. Comput. 168 (2005) 962–972, doi:10.1016/j.amc.2004.09.027.
[8] A.A. Soliman, Numerical simulation of the generalized regularized long wave equation by He's variational iteration method, Math. Comput. Simul. 70 (2005) 119–124, doi:10.1016/j.matcom.2005.06.002.
[9] J.I. Ramos, Solitary wave interactions of the GRLW equation, chaos, Solitons Fractals 33 (2007) 479–491, doi:10.1016/j.chaos.2006.01.016.
[10] H. Jafari, A. Borhanifar, S.A. Karimi, New solitary wave solutions for generalized regularized long-wave equation, Int. J. Comput. Math. 87 (3) (2010) 509–514, doi:10.1080/00207160802123441.
[11] R. Mokhtari, M. Mohammadi, Numerical solution of GRLW equation using sinc-collocation method, Computer Physics Communications 181 (2010) 1266–1274, doi:10.1016/j.cpc.2010.03.015.

[12] M. Mohammadi, R. Mokhtari, Solving the generalized regularized long wave equation on the basis of a reproducing kernel space, J. Comput. Appl. Math. 235 (2011) 4003–4014, doi:10.1016/j.cam.2011.02.012.
[13] T. Roshan, A Petrov-Galerkin method for solving the generalized regularized long wave (GRLW) equation, Comput. Math. Appl. 63 (2012) 943–956, doi:10.1016/j.camwa.2011.11.059.
[14] C.M. Garcia-Lopez, J.I. Ramos, Effects of convection on a modified GRLW equation, Appl. Math. Comput. 219 (2012) 4118–4132, doi:10.1016/j.amc.2012.10.066.
[15] R. Akbari, R. Mokhtari, A new compact finite difference method for solving the generalized long wave equation, Numer. Funct. Anal. Optim. 35 (2) (2014) 133–152, doi:10.1080/01630563.2013.830128.
[16] D.M. Huang, L.W. Zhang, Element-free approximation of generalized regularized long wave equation, Math. Probl. Eng. 2014 (2014) 1–10, doi:10.1155/2014/206017.
[17] T.S. EL-Danaf, K.R. Raslan, K.K. Ali, New numerical treatment for the generalized regularized long wave equation based on finite difference scheme, Int. J. Soft Comput. Eng. 4 (4) (2014) 16–24.
[18] P.F. Guo, L.W. Zhang, K.M. Liew, Numerical analysis of generalized regularized long wave equation using the element-free kp-Ritz method, Appl. Math. Comput. 240 (2014) 91–101, doi:10.1016/j.amc.2014.04.023.
[19] D.A. Hammad, M.S. El-Azab, A 2n order compact finite difference method for solving the generalized regularized long wave (GRLW) equation, Appl. Math. Comput. 253 (2015) 248–261, doi:10.1016/j.amc.2014.12.070.
[20] L.R.T. Gardner, G.A. Gardner, I. Dag, A b-spline finite element method for the regularized long wave equation, Commun. Numer. Methods Eng. 11 (1) (1995) 59–68, doi:10.1002/cnm.1640110109.
[21] K.R. Raslan, Collocation method using quadratic b-spline for the RLW equation, Int. J. Comput. Math. 78 (3) (2001) 399–412.
[22] I. Dag, B. Saka, D. Irk, Application of cubic b-splines for numerical solution of the RLW equation, Appl. Math. Comput. 159 (2) (2004) 373–389, doi:10.1016/j.amc.2003.10.020.
[23] A.A. Soliman, M.H. Hussien, Collocation solution for RLW equation with septic spline, Appl. Math. Comput. 161 (2) (2005) 623–636, doi:10.1016/j.amc.2003.12.053.
[24] B. Saka, I. Dag, D. Irk, Quintic b-spline collocation method for numerical solution of the RLW equation, ANZIAM J. 49 (3) (2008) 389–410, doi:10.1017/S1446181108000072.
[25] B. Saka, A. Sahin, I. Dag, B-spline collocation algorithms for numerical solution of the RLW equation, Numer. Methods Partial Differ. Equ. 27 (3) (2011) 581–607, doi:10.1002/num.20540.
[26] L.R.T. Gardner, G.A. Gardner, F.A. Ayoub, N.K. Amein, Approximations of solitary waves of the MRLW equation by b-spline finite element, Arab. J. Sci. Eng. 22 (1997) 183–193.
[27] A.K. Khalifa, K.R. Raslan, H.M. Alzubaidi, A collocation method with cubic b-splines for solving the MRLW equation, J. Comput. Appl. Math. 212 (2) (2008) 406–418, doi:10.1016/j.cam.2006.12.029.
[28] K.R. Raslan, T.S. EL-Danaf, Solitary waves solutions of the MRLW equation using quintic b-splines, J. King Saud Univ. Sci. 22 (3) (2010) 161–166, doi:10.1016/j.jksus.2010.04.004.
[29] F. Haq, S. Islam, I.A. Tirmizi, A numerical technique for solution of the MRLW equation using quartic b-splines, Appl. Math. Model. 34 (12) (2010) 4151–4160, doi:10.1016/j.apm.2010.04.012.
[30] I. Dag, D. Irk, M. Sari, The extended cubic b-spline algorithm for a modified regularized long wave equation, Chin. Phys. B 22 (4) (2013), doi:10.1088/1674-1056/22/4/040207.
[31] S.B.G. Karakoç, N.M. Yagmurlu, Y. Ucar, Numerical approximation to a solution of the modified regularized long wave equation using quintic b-splines, Bound. Value Probl. 2013 (2013) 27, doi:10.1186/1687-2770-2013-27.
[32] S.B.G. Karakoç, T. Ak, H. Zeybek, An efficient approach to numerical study of the MRLW equation with b-spline collocation method, Abstr. Appl. Anal. 2014 (2014) 1–15, doi:10.1155/2014/596406.
[33] S.G. Rubin, R.A. Graves, A Cubic Spline Approximation for Problems in Fluid Mechanics, Washington DC, 1975. NASA TR R-436.
[34] M. Dumbser, M. Facchini, A space-time discontinuous Galerkin method for Boussinesq-type equations, Appl. Math. Comput. 272 (2016) 336–346, doi:10.1016/j.amc.2015.06.052.